

# Adaptation of frequency-domain readout for Transition Edge Sensor bolometers for the POLARBEAR-2 Cosmic Microwave Background experiment

Kaori Hattori<sup>a</sup>, Kam Arnold<sup>c</sup>, Darcy Barron<sup>c</sup>, Matt Dobbs<sup>d</sup>, Tijmen de Haan<sup>d</sup>, Nicholas Harrington<sup>b</sup>, Masaya Hasegawa<sup>a</sup>, Masashi Hazumi<sup>a</sup>, William L. Holzapfel<sup>b</sup>, Brian Keating<sup>c</sup>, Adrian T. Lee<sup>b</sup>, Hideki Morii<sup>a</sup>, Michael J. Myers<sup>b</sup>, Graeme Smecher<sup>e</sup>, Aritoki Suzuki<sup>b</sup>, Takayuki Tomaru<sup>a</sup>

<sup>a</sup>High Energy Accelerator Research Organization (KEK), Tsukuba, Japan

<sup>b</sup>University of California, Berkeley, Physics, Berkeley, CA, USA

<sup>c</sup>University of California, San Diego, La Jolla, CA, USA

<sup>d</sup>McGill University, Montreal, Quebec, Canada

<sup>e</sup>Three-Speed Logic, Inc., Vancouver, Canada

arXiv:1306.1869v2 [astro-ph.IM] 4 Jul 2013

---

## Abstract

The POLARBEAR-2 Cosmic Microwave Background (CMB) experiment aims to observe B-mode polarization with high sensitivity to explore gravitational lensing of CMB and inflationary gravitational waves. POLARBEAR-2 is an upgraded experiment based on POLARBEAR-1, which had first light in January 2012. For POLARBEAR-2, we will build a receiver that has 7,588 Transition Edge Sensor (TES) bolometers coupled to two-band (95 and 150 GHz) polarization-sensitive antennas. For the large array's readout, we employ digital frequency-domain multiplexing and multiplex 32 bolometers through a single superconducting quantum interference device (SQUID). An 8-bolometer frequency-domain multiplexing readout has been deployed on POLARBEAR-1 experiment. Extending that architecture to 32 bolometers requires an increase in the bandwidth of the SQUID electronics to 3 MHz. To achieve this increase in bandwidth, we use Digital Active Nulling (DAN) on the digital frequency multiplexing platform. In this paper, we present requirements and improvements on parasitic inductance and resistance of cryogenic wiring and capacitors used for modulating bolometers. These components are problematic above 1 MHz. We also show that our system is able to bias a bolometer in its superconducting transition at 3 MHz.

**Keywords:** TES bolometer, digital feedback, frequency-domain multiplexing, Cosmic Microwave Background, POLARBEAR-2

---

## 1. Introduction

The POLARBEAR experiment [1] aims to observe the B-mode polarization pattern imprinted on the cosmic microwave background (CMB). The B-mode polarization, not discovered yet, is a powerful tool for exploring gravitational lensing of CMB and inflationary gravitational waves [2]. The POLARBEAR-1 experiment had first light in January 2012 at 5150 meters altitude in the Atacama Desert [4] [5]. Scientific observations have been ongoing with 1,274 single band (150 GHz) antenna-coupled, polarization sensitive Transition Edge Sensor (TES) bolometers.

POLARBEAR-2 is an upgraded experiment, which will be more sensitive to the B-mode and E-mode polarization signals [3]. We will build a receiver that has 7,588 TES bolometers coupled to two-band (95 and 150 GHz) polarization-sensitive antennas [6]. The kilopixel arrays of multi-band polarization-sensitive pixels are necessary to achieve the high sensitivity required by these science goals. Multiband observations were chosen to mitigate the foreground produced by synchrotron radiation and dust emission.

For TES bolometer array readout, we employ digital frequency-domain multiplexing (fMUX) [7] and multiplex bolometers through a single superconducting quantum interference device (SQUID) mounted on the 4 K stage. Each TES

bolometer ( $R_{bolo}$ ) is connected to an inductor ( $L$ ) and a capacitor ( $C$ ) in series to define a frequency of its voltage-bias carrier, shown in Fig. 1. An 8-bolometer fMUX readout has been deployed on the POLARBEAR-1 experiment. The fMUX readout has been also deployed on the APEX-Sunyaev-Zeldovich (SZ) [8] and South Pole Telescope (SPT) SZ [9] which have 7x multiplexing, SPT pol with 12x [10], and EBEX with 16x [11]. Polarbear-2 will employ 32x multiplexing to read out its large number of detectors. In the following section, we describe the requirements imposed by this high multiplexing factor.

## 2. Improvements for readout

### 2.1. Bandwidth

Extending that architecture to 32 bolometers requires an increase in the bandwidth of the SQUID electronics. The bandwidth is determined by spacing of resonances defined by LC filters. The spacing is chosen such that cross talk from adjacent resonance is small in comparison to the other sources of cross talk in the experiment. For POLARBEAR-2 a spacing of 90 kHz will be used and the total bandwidth will be 3 MHz. The spacing is similar to that chosen for POLARBEAR-1. Because of the limited dynamic range of the SQUID, the POLARBEAR-1 readout used a broadband analog feedback loop [12], which

is limited to 1 MHz due to phase delay from the 300 K to 4 K wiring. To overcome this limitation, we use an alternative feedback technique called Digital Active Nulling (DAN) [13] on the digital frequency multiplexing platform. With DAN, digital feedback is calculated across the narrow bandwidth of each bolometer, extending the useful bandwidth of the SQUID amplifier.

## 2.2. Parasitic inductance

### 2.2.1. SQUID and wiring impedance

A strong constraint on the readout with the high bandwidth is cross talk induced by the parasitic inductances of the SQUID input coil and the wiring. They are shown at  $L_{squid}$ ,  $L_1$  and  $L_2$  in Fig. 1 (a). The current at resonant frequency  $\omega_i = 1/\sqrt{LC_i}$  flows not only through the  $i$ th bolometer but also into the  $i \pm 1$ th channels. The voltage drop across the parasitic inductance modulates  $i \pm 1$  channels and causes cross talk. The power fluctuation of channel  $i$  bolometer,  $dP_i^{\omega_i}$ , induces cross talk on the neighboring bolometers [12],

$$\frac{dP_{i\pm 1}^{\omega_i}}{dP_i^{\omega_i}} \simeq -\frac{I_{i\pm 1}^{\omega_i}}{I_i^{\omega_i}} \frac{\omega_i L_s}{\Delta\omega L}, \quad (1)$$

where  $I_i^{\omega_i}$  is the current flowing through channel  $i$  bolometer,  $L_s$  is sum of the parasitic inductance,  $L_s = L_1 + L_2 + L_{squid}$ , and  $\Delta\omega$  is the frequency spacing. Equation (1) implies that the parasitic inductance should be inversely proportional to the bandwidth to maintain the cross talk at the same level.

The parasitic inductance  $L_s$  also affects the bolometer stability. In the limit of infinite channel spacing, it shifts the resonant frequency. At the resonant frequency  $\omega_i = 1/\sqrt{(L + L_s)C_i}$ , there is no effective series impedance. With finite spacing,  $L_s$  cannot be removed completely due to the current flowing through the neighboring channels. The effective series impedance is approximately the ratio of parasitic inductance to channel spacing. If it becomes comparable with the bolometer resistance ( $\sim 1\Omega$ ), it deteriorates the bolometer stability. The situation becomes worse as the carrier frequency increases. Since the bandwidth used for POLARBEAR-2 readout is three times larger, the parasitic inductance should be suppressed by 1/3 to avoid degradation of the performance.

### 2.2.2. Suppression of parasitic inductance

The parasitic inductance  $L_1$  and  $L_2$  shown in Fig. 1 (a) arises from the cryogenic wiring that connects the bias resistor at 4 K to the LC filters at 0.3 K.

For POLARBEAR-1, the bias resistor is mounted on the 4 K stage, which is far from the 0.3 K stage where the LC filters are mounted. The cable used for POLARBEAR-1 consists of two segments; a 64-cm low inductance broadside coupled stripline which has high thermal conductivity, and a 10-cm high-inductance NbTi twisted pair which is necessary to achieve thermal isolation between 4 K and 0.3 K. Total parasitic inductance coming from the cable is  $1.0 \text{ nH/cm (stripline)} \times 64 \text{ cm} + 7.0 \text{ nH/cm (twisted cables)} \times 10 \text{ cm} = 134 \text{ nH}$ . For POLARBEAR-2, it should be suppressed by 1/3, below 45 nH. We have been developing a low inductance NbTi broadside

coupled stripline for thermal break. Assuming an inductance of  $1.0 \text{ nH/cm}$  and the current cable length of 74 cm, the parasitic inductance would be 74 nH, which is much larger than the requirement. The distance between the LC filters and the bias resistor should be shorter than 45 cm.

To solve this issue, we will move the bias resistors closer to the  $LCR_{bolo}$  circuit and enclose the majority of the parasitic inductance in the DAN loop, as shown in Fig. 1 (b). DAN nulls current flowing in the DAN loop, shown in the highlighted line in Fig. 1 (b), effectively reducing the parasitic inductance and the input impedance of the SQUID. The long SQUID input lines would not be suitable for the analog Flux locked loop used in POLARBEAR-1. It can work well with the DAN system, wherein the feedback occurs only in narrowband lines around the bolometer bias frequency.

Ideally, the bias resistor should be placed to next to the  $LCR_{bolo}$  circuit to minimize  $L_1$  and  $L_2$ . The position of the bias resistors is determined by the cooling power of the cryostat. Total power dissipation of the bias resistors will be  $2.5 \mu\text{W}$ , which is similar to the cooling power of the 0.25 K stage. The bias resistor should be placed at 0.35 K, which have more than 25 times cooling power in our cryogenic system. The bias resistor can be mounted on the NbTi broadside coupled stripline connecting 0.25 K and 4 K and can be thermally linked to the 0.35 K stage by heat strap. This setup can circumvent the limitation on the wiring length of 45 cm. Another solution is to use a bias inductor that has no power dissipation and can be mounted on the 0.25 K stage. An advantage for this setup is that  $L_1$  and  $L_2$  will be negligible. A disadvantage is that it will have three times its number of cables running to the 0.25 K stage. The thermal flow through these cables and the limited space around the 0.25 K stage might be problematic.

## 2.3. Capacitors

### 2.3.1. Equivalent Series Resistance

Another stray impedance that spoils the voltage bias across the bolometer is the equivalent series resistance (ESR) of the capacitors that form the  $LCR_{bolo}$  circuit. Ideally, the ESR should be smaller than about  $0.1 \Omega$  ( $0.1R_{bolo}$ ). Assuming that the inductance  $L$  is constant and the capacitance  $C$  is used to select the frequency  $f$ , the contribution of the dielectric loss to ESR is a linear function of frequency,  $R_{ESR} = 2\pi L f \tan \delta$ , where  $\tan \delta$  is the loss tangent of the dielectric material. For the high frequency readout, material having low loss tangent should be used. To have  $R_{ESR} < 0.1\Omega$  at 3 MHz, loss tangent should be  $< 2.2 \times 10^{-4}$ . For POLARBEAR-1, commercial surface mount multi-layer ceramic capacitors were used. We investigated their usability for POLARBEAR-2.

Figure 2 shows a block diagram of ESR measurement setup. Each capacitor is connected to a niobium inductor in series which forms LC filter. We used  $24\text{-}\mu\text{H}$  inductors that will be used for POLARBEAR-2. The setup was cooled to 4.2 K using  $^4\text{He}$ .

At resonant frequency, the resistors  $R_0$  and  $R_{ESR}$  shown in Fig. 2 form a voltage divider. ESR is measured by frequency-sweeping a probe signal, monitoring  $V_{in}$  and  $V_{out}$ , and measur-

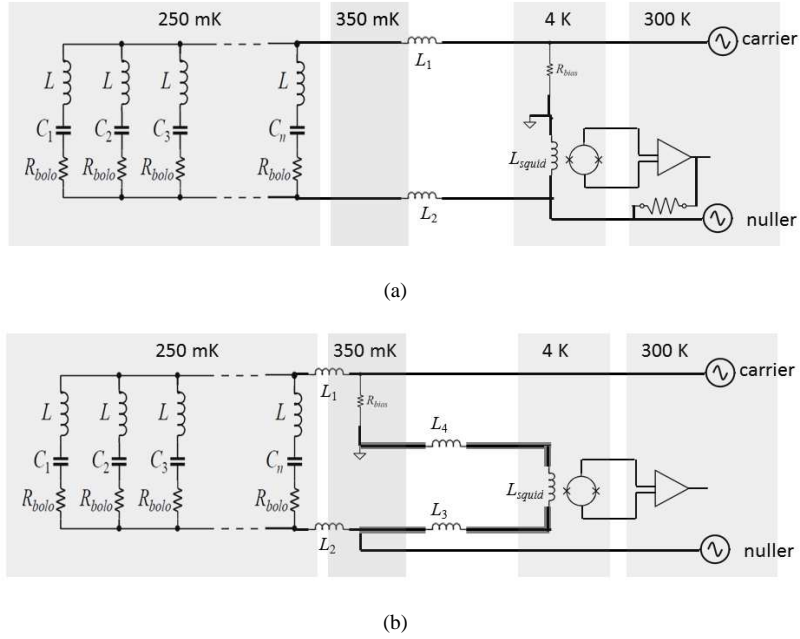


Figure 1: Block diagrams showing the digital fMUX readout of (a) POLARBEAR-1. The resistor applying voltage bias across the bolometer is placed next to the SQUID at 4 K. The parasitic inductance of the wiring shown at  $L_1$  and  $L_2$  spoils the voltage bias. (b) For POLARBEAR-2, the resistor will move closer to the  $LCR_{bolo}$  circuit. The majority of the parasitic inductance of the wiring shown at  $L_3$  and  $L_4$  is enclosed in the DAN loop, shown at the highlighted line.

ing the peak height of each LC resonance. To eliminate resistance of cables running from room temperature to 4 K,  $R_1$ , and  $V_{out}/V_{in}$  are also measured. The series resistance without a capacitor was  $0.020 \Omega$ .

We have tested a wide variety of commercial surface mount multi-layer ceramic capacitors. In Fig. 3, data points above 1 MHz show the best ESR we have obtained so far. High-Q, low-loss capacitors made by Vishay Vitramon and Johanson Technology Inc. were stacked in parallel to achieve the target capacitance. The plots below 1 MHz are ESRs of the capacitors used for POLARBEAR-1. As expected from the loss tangent, the ESR is high at high frequency. The fluctuation of the ESRs are due to the stacked capacitors. They were made from capacitors of different brands and processes, resulting different properties. The ESR depends on not only the capacitance but also brands. The ESR is acceptable below 1 MHz while it doesn't meet the requirement above 1 MHz. We will investigate lower ESR capacitors.

### 2.3.2. Capacitance accuracy

It is important to set the bias frequencies with a constant spacing in order to avoid cross talk, such as shown by Eq. (1). Inductors we have used were fabricated at the National Institute for Standards and Technology (NIST), with a lithographic process. We are able to obtain sufficient uniformity by lithography. With the high bandwidth readout, capacitance accuracy is essential. At the highest frequency of 3 MHz, the accuracy should be 0.6 % assuming the error of the bias frequency is 10 % (9 kHz). The capacitance accuracy of commercial surface mount ceramic capacitors is typically worse than 1 %. Since most of channels have stacked capacitors in parallel, the to-

tal error could be larger. For the best devices, the capacitance changes by several per cent or more after being cooled from room temperature to sub-Kelvin.

To solve this issue, we will investigate lithographed capacitors. The lithographic process is expected to control relative capacitances well. Though the lithographed capacitors could have large deviation from the design capacitance value, the absolute frequencies are much less important than the relative frequencies in terms of cross talk. One candidate is parallel-plate capacitors having superconducting plates separated by low loss tangent dielectric. SRON has demonstrated such capacitors [14]. Another candidate are interdigitated capacitors [15] formed on a low loss material. Lumped Element Kinetic Inductance Detectors [16] having resonant frequencies of a few GHz utilize interdigitated capacitors, which should have low loss. Since there is no thin film involved in the design, they will be less susceptible to ESD (electrostatic discharges), which is often an issue with thin film capacitors.

## 3. High frequency Multiplexing testing

We have demonstrated high-frequency readout shown in Fig. 1 (b). For LC filters,  $24\text{-}\mu\text{H}$  inductors fabricated by NIST and the capacitors whose ESRs are shown in Fig. 3 were used. The majority of parasitic impedance is enclosed in the DAN loop. The ratio is approximately  $(L_1 + L_2) : (L_3 + L_4) = 1 : 25$ . Figure 4 shows bolometer resistance vs. power for a bolometer voltage-biased at 3.10 MHz. The bolometer is operated dark at a bath temperature of 0.38 K. As the bias voltage was reduced, the device fell into transition and held the power applied across the bolometer by electro-thermal feedback (ETF).

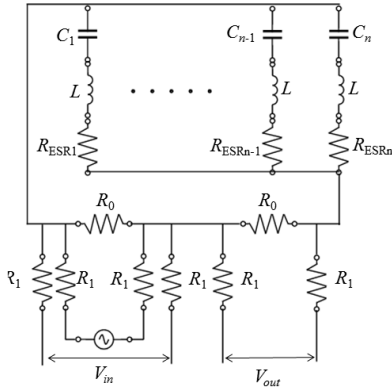


Figure 2: Block diagram showing equivalent series resistance (ESR) measurement setup.

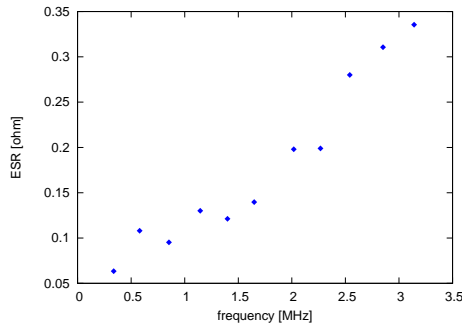


Figure 3: Equivalent series resistance (ESR) of commercial surface mount multi-layer ceramic capacitors measured at liquid  $^4\text{He}$  temperature (4 K).

#### 4. Future developments

We have shown that we can bias bolometers in their transition at 3 MHz. To maintain the performance of TES bolometers at high frequency, we will investigate low ESR capacitors. Capacitance accuracy will be important for large focal planes such as that of POLARBEAR-2 to obtain high yield. Lithographed capacitors will be expected to improve the yield.

We have been designing components for 32x multiplexing: (1) a low inductance NbTi broad-side coupled stripline having a bias resistor on it, and (2) a SQUID mounting board that has SQUIDS at 4 K. The new board will have three pairs of wires between the 4K SQUID and the sub-Kelvin bolometers; a carrier line, a nuller line and a return line. This differs from the existing SQUID board that was used for POLARBEAR-1 which had only a single pair of wires providing the bolometer bias and return. In future work, we will examine the performance of a high-bandwidth readout system with both the newly developed components and bolometers fabricated for the POLARBEAR-2 experiment.

#### 5. Acknowledgement

The POLARBEAR-2 experiment is funded by a Grant-in-Aid for Scientific Research from the Japan Society for the Promotion of Science, and the National Science Foundation AST-

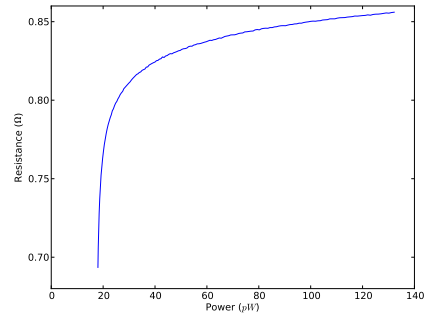


Figure 4: Bolometer resistance vs. power for a bolometer voltage-biased at 3.10 MHz.

1207892 of the United States of America. The McGill authors acknowledge funding from the Natural Sciences and Engineering Research Council and Canadian Institute for Advanced Research. All TES bolometers are fabricated at the UC Berkeley Microlab. We thank NIST for design/fabrication of niobium inductors.

#### References

- [1] B. Keating et al., arXiv:1110.2101 (2011).
- [2] H. C. Chiang et al., APJ, 711 (2010) 1123.
- [3] T. Tomaru et al., Proc. SPIE 8452, Millimeter, Submillimeter, and Far-Infrared Detectors and Instrumentation for Astronomy VI, (2012) 84521H.
- [4] Z. Kermish et al., Proc. SPIE 8452, Millimeter, Submillimeter, and Far-Infrared Detectors and Instrumentation for Astronomy VI, (2012) 84521C.
- [5] K. Arnold et al., Proc. SPIE 8452, Millimeter, Submillimeter, and Far-Infrared Detectors and Instrumentation for Astronomy VI, (2012) 84521D.
- [6] A. Suzuki et al., Proc. SPIE 8452, Millimeter, Submillimeter, and Far-Infrared Detectors and Instrumentation for Astronomy VI, (2012) 84523H.
- [7] M. A. Dobbs et al., J. Low. Temp. Phys. 167 (2012) 568.
- [8] M. A. Dobbs et al., New Astron. Rev. 50 (2006) 960.
- [9] J. E. Carlstrom et al., Publ. Astron. Soc. Pac. 123 (2011) 568.
- [10] J. E. Austermann et al., Proc. SPIE 8452, Millimeter, Submillimeter, and Far-Infrared Detectors and Instrumentation for Astronomy VI, (2012) 84520E.
- [11] B. Reichborn-Kjennerud et al., Proc. of SPIE 7741 (2010) 77411C.
- [12] M. A. Dobbs et al., Rev. Sci. Instrum. 83 073113 (2012) 073113.
- [13] T. de Haan et al., Proc. SPIE 8452, Millimeter, Submillimeter, and Far-Infrared Detectors and Instrumentation for Astronomy VI, (2012) 845213.
- [14] M. P. Bruijn et al., J. Low. Temp. Phys. 167 (2012) 695.
- [15] I. J. Bahl "Lumped Elements For Rf And Microwave Circuits" Artech House.
- [16] S. Doyle et al., J. Low. Temp. Phys. 151 (2008) 530.